4532 *Macromolecules* **2010**, *43*, 4532–4542
DOI: 10.1021/ma1002672

Macromolecules
ARTICLE

Penultimate Effects and Chain Epimerization in Propene−Norbornene Copolymers by *rac*-$Me_2Si(2\text{-}Me\text{-}Ind)_2ZrCl_2$ C_2-Symmetric Metallocene

Laura Boggioni, Andrea Ravasio, Cristina Zampa, Dino Romano Ferro, and Incoronata Tritto*

Istituto per lo Studio delle Macromolecole, Consiglio Nazionale delle Ricerche, Via E. Bassini 15, I-20133 Milano, Italy

Received February 3, 2010; Revised Manuscript Received April 9, 2010

ABSTRACT: The copolymerization of propene (P) and norbornene (N) by the catalytic system composed of *rac*-$Me_2Si(2\text{-}Me\text{-}Ind)_2ZrCl_2$ (**3**) and methylaluminoxane (MAO) was investigated and compared with that by *rac*-$Et(Ind)_2ZrCl_2$ (**1**) and MAO. Methyl 2 substitution on the indenyl ligand in **3** has an unexpected and strong influence on the catalyst behavior in P−N copolymerization, causing a strong decrease in catalytic activity, molar fraction f_N, T_g, and M_n values. P−N copolymers with maximum of 16 mol % of norbornene were obtained by **3-MAO** in contrast with those highly alternating obtained by **1-MAO**. The microstructural analysis by ^{13}C NMR of the copolymers at triad level and reactivity ratios r_i and r_{ij} obtained from diads and triads, respectively, give evidence of the tendency to alternate or not to alternate P and N comonomers and information on the probability of insertions of N and of the possible forms of P insertions (P_{12}, P_{13}, and P_{21}). Penultimate effects were demonstrated as **3-MAO** has difficulty in accommodating a norbornene into Mt-P_{12}N and Mt-P_{13}N bonds. A great decrease in the tacticity of the PP blocks in copolymers prepared with **3-MAO** when increasing norbornene content in the feed revealed the high probability of $R-S$ isomerization of the last inserted propene. Chain end groups analysis showed a greater amount of 2-butenyl end groups arising from termination at a Mt-P_{21} than of vinylidene arising from termination at a Mt-P_{12}. This is an evidence that the limiting step in P−N copolymerization is the difficulty to insert a propene after N, which causes 2,1 insertions with subsequent isomerization to 1,3 propene insertions. This effect also originates chain epimerization under starved propene conditions with catalyst **3-MAO**.

Introduction

Cyclic olefin copolymers (COCs) made available by *ansa*-metallocene catalysts have experienced a great interest in academia and industries.[1−9] Indeed, they are a new interesting class of amorphous and thermoplastic materials with high glass-transition temperatures (T_g). They show excellent transparency and high refractive index because of their rigid bicyclic monomer units, high chemical resistance, low water absorption, good solubility in organic solvents, and good processability. TAP (formerly Ticona and Hoechst) has developed the ethene (E)−norbornene (N) copolymers, the most versatile and interesting ones, to commercial products. They display a wide range of T_g values from room temperature to ∼220 °C.

The incorporation of norbornene into the isotactic polypropene chain was expected to be endowed with higher T_g than E−N copolymers with the same N content and molar mass (M_w) because polypropene (PP) has a higher T_g than polyethene. Differences in stereo- and regioregularity of propene units as well as in the comonomer distribution and the stereoregularity of the bicyclic units would allow us to tune copolymer properties. Such differences originate complex microstructures of the polymer chain and complex ^{13}C NMR spectra.[10−14] Therefore, interpretation of P−N copolymer spectra is much more difficult than that of E−N copolymers. We tackled the synthesis and microstructural studies of P−N copolymers with two C_2-symmetric metallocenes *rac*-$Et(Ind)_2ZrCl_2$ (**1**) and *rac*-$Me_2Si(Ind)_2ZrCl_2$ (**2**) (Chart 1) and methylaluminoxane (MAO) as cocatalyst.[11] ^{13}C NMR experiments and ab initio theoretical chemical shift calculations, combined with RIS statistics of the P−N chain, gave the first assignment of the ^{13}C NMR spectra of P−N copolymers.[11] More recently, the influence of propene pressure and temperature on activity, norbornene content, M_w, and T_g of P−N copolymers by **1-MAO** was assessed.[12] A decrease in norbornene content, M_w, and T_g was observed at high temperature and pressure. The great number of 1,3 propene insertions found especially at high temperature and pressure, occurring after an inserted norbornene unit, indicated that the limiting step in P−N copolymerization is the difficulty to insert a P after N. Moreover, chain transfer reactions are likely to occur more often at a P-last inserted-Mt bond: indeed, chain transfer reactions at a Mt-N bond are rather difficult because the β−H transfer would violate Bredt's rule, that is, the coplanarity of Zr−C(α)−C(β)−H.

Chart 1. C_2 Symmetric Metallocenes under Investigation: *rac*-$Et(Ind)_2ZrCl_2$ (1) and *rac*-$Me_2Si(2\text{-}Me\text{-}Ind)_2ZrCl_2$ (3)

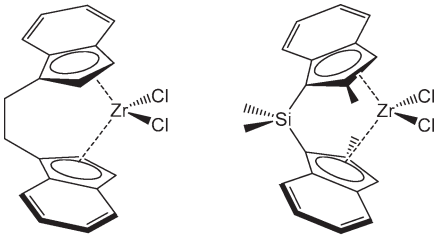

1 3

The M_w values of the P−N copolymers are quite low in comparison with those of E−N copolymers. The highest molar masses obtained at room temperature were in the range of 40 000 Da. For mechanical properties and processability requirements,

*Corresponding author. E-mail: i.tritto@ismac.cnr.it.

 Published on Web 04/30/2010 © 2010 American Chemical Society

Table 1. Polymerization Conditions and Copolymers Obtained with Propene - Norbornene Copolymerizations with the Catalysts *rac*-Et-(Ind)$_2$ZrCl$_2$ (1) and *rac*-Me$_2$Si(2-Me-Ind)$_2$ZrCl$_2$ (3)[a]

catalyst	entry	[N]/[P] feed	f_N[b]	activity (kgpol/molZr·h)	time (h)	T_g (°C)	$M_n \times 10^{-3}$ (g/mol)	M_w/M_n[c]
3	1	0.00	0.00	123 180	0.05	n.d.	n.d.	n.d.
3	2	0.05	0.12	1480	0.25	0.4	15.5	2.0
3	3	0.10	0.16	180	0.58	12	7.1	2.4
3	4	0.13	0.15	60	1.17	10	7.4	1.9
3	5	0.29	0.16	30	1.25	22	5.0	3.7
1	6	0.00	0.00	6140	0.33	n.d	n.d.	n.d.
1	7	0.06	0.22	400	0.67	39	4.0	1.6
1	8	0.11	0.34	170	1.50	80	11.1	1.9
1	9	0.22	0.41	50	2.00	104	15.1	1.9
1	10	0.42	0.45	20	2.50	113	13.7	1.9
1	11	0.53	0.45	10	2.50	121	13.5	1.7

[a] Polymerization conditions: total volume in toluene = 350 mL, pP = 5 bar, 40 °C, cocatalyst = dried MAO + Al^{i}Bu$_3$, [Al$_{tot}$]/[Zr] = 2000, [Zr] = 10^{-4} mol/L. [b] Fraction of norbornene incorporated in the copolymer calculated from ^{13}C NMR spectra.[18] [c] Determined by SEC relative to polystyrene standards.

polymer molar masses must be in the range 40 000−300 000 at current plant polymerization temperatures (60−80 °C).

Chain transfers in propene polymerization from metallocenes include β-hydride transfer to the metal and β-hydride transfer to the monomer.[15] They are dictated from metallocene ligands and depend on the polymerization temperature, type of cocatalyst, and propene concentration. Because the 2-alkyl indenyl substitution of C_2-symmetric zirconocenes is key in increasing considerably the molar masses of the produced polymers, we envisioned that *rac*-Me$_2$Si(2-Me-Ind)$_2$ZrCl$_2$ (**3**) (Figure 1) could enable the synthesis of P−N copolymers with high norbornene content and high molar masses.[16]

The aim of this work is to investigate P−N copolymerization with the C_2 symmetric catalyst *rac*-Me$_2$Si(2-Me-Ind)$_2$ZrCl$_2$ (**3**), which is able to incorporate high amounts of N in NNN blocks.[17] A comparison with the results obtained with *rac*-Et(Ind)$_2$ZrCl$_2$ under the same conditions would allow us to evaluate the effect of the substituent on the indenyl ligand on the catalyst behavior in P−N copolymerization because previous results revealed that the different bridge in *rac*-Et(Ind)$_2$ZrCl$_2$ (**1**) and *rac*-Me$_2$Si(Ind)$_2$ZrCl$_2$ has a small influence on catalytic activity, molar fractions, f_N, T_g, and M_n values. A more detailed microstructural analysis by ^{13}C NMR of such copolymers was necessary and is the object of a recent paper.[18] Such an analysis of the spectra allowed us to determine the molar fractions of the sequences defining the microstructure of a P−N copolymer at triad level. Here the microstructural and chain end groups analysis and the molecular and thermal characterization of the copolymers are presented. On the basis of the copolymer microstructure, relative reactivity and intramolecular distribution of the comonomers were expressed by reactivity (Chart 2) ratios r_i and r_{ij}. All results are discussed to get insight into olefin polymerization mechanisms operating in these systems.

Results and Discussion

Synthesis and Characterization of Copolymers. Series of propene and norbornene copolymerizations were performed by **3-MAO** at [Al]/[Zr] molar ratio of 2000 in toluene at 40 °C at 5 bar pressure of propene, that is, under the conditions optimal for balancing chain propagation of the two competing comonomers and chain termination with **1-MAO**. A range of [N]/[P] feed ratios as wide as possible was investigated. The polymerization tests were designed to study copolymer microstructure, that is, low comonomer conversion and low polymer concentration in the polymerization medium. Norbornene conversion was kept below 10%. The norbornene content in the copolymer was calculated by the analysis of ^{13}C NMR spectra by the procedure reported in the reference18. Glass-transition temperatures and molar masses were estimated by DSC and size exclusion chromatography (SEC) measurements, respectively. The results concerning the synthesis and the characterization of selected copolymers are summarized in Table 1, where they are compared with those of a series of P−N copolymerizations with **1-MAO** under the same conditions. The catalytic system **3-MAO** showed high activity for polypropene (4 times higher than with *rac*-Et(Ind)$_2$ZrCl$_2$), as expected. As in almost all N copolymerizations by *ansa*-metallocenes, the increase in N concentration in the polymerization feed results in a decrease in catalytic activity (Chart 3), likely because of the facility of N coordination to the active sites. Surprisingly, polymerization activity with **3-MAO** drops in the presence of norbornene at rather low [N]/[P] feed ratios: it was not possible to obtain P−N copolymer samples at a ratio between norbornene and propene in feed higher than 0.3 under these conditions.

Chart 2. Typical Random P−N Copolymer Chain

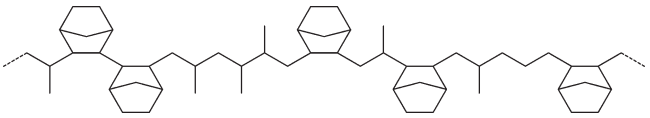

Therefore, whereas *rac*-Me$_2$Si(2-Me-Ind)$_2$ZrCl$_2$ is much more active for PP production than *rac*-Et(Ind)$_2$ZrCl$_2$, the two catalytic systems have quite similar catalytic behavior for P−N copolymerization at [N]/[P] feed ratios between 0.05 and 0.3, as shown in Chart 3, where the activity values obtained are compared. In contrast, at higher [N]/[P] ratios in feed, polymer products could not be obtained with **3-MAO**.

The norbornene contents incorporated in the copolymer chain by catalysts **1-MAO** and **3-MAO,** compared in Chart 4, show a typical increase in N content in the copolymer with [N]/[P] ratios up to a plateau. The catalytic ability to insert norbornene is clearly different: the molar fraction of norbornene (f_N) incorporated by **3-MAO** is much lower than that by **1-MAO**, especially at higher [N]/[P] ratios. Indeed, the maximum value obtained is an f_N of 0.12 for an [N]/[P] of 0.29, similar to that obtained at an [N]/[P] of 0.10, whereas for *rac*-Et(Ind)$_2$ZrCl$_2$ at [N]/[P] of about 0.11 the f_N value is 0.34 and the maximum value is 0.45. These differences are surely due to the presence of the methyl substituent on the indenyl of **3**: the bulkier ligand around the metal center probably makes more difficult the insertion of the propene in the polymer chain after the bulky norbornene. Moreover, being f_N well below 0.5, the norbornene concentration in the feed (or its coordination to the metal center) should play a role in the norbornene incorporation in the polymer chain as well as in the activity.

Chart 3. Plot of Activity Values for P−N Copolymers Obtained with *rac*-Et(Ind)$_2$ZrCl$_2$ and *rac*-Me$_2$Si(2-Me-Ind)$_2$ZrCl$_2$ at 5 bar, 40 °C versus [N]/[P] in the Feed

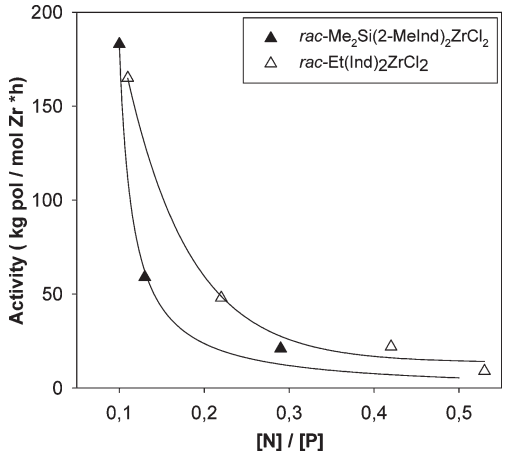

Chart 4. Plot of Norbornene Content for P−N Copolymers Obtained with *rac*-Et(Ind)$_2$ZrCl$_2$ and *rac*-Me$_2$Si(2-Me-Ind)$_2$ZrCl$_2$ at 5 bar, 40 °C versus [N]/[P] in the Feed

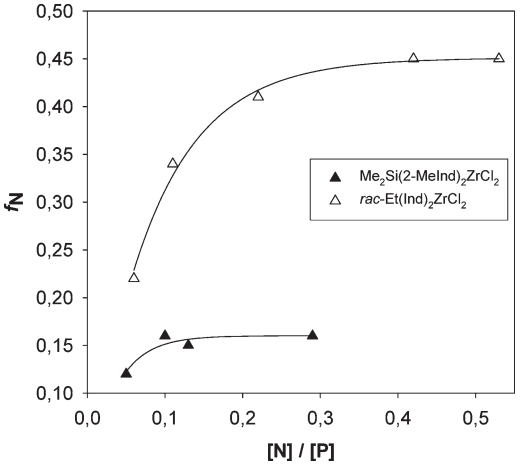

The molar masses have been investigated by SEC. Molar-mass distributions (M_w/M_n) are in general characteristic of single-site catalytic systems. Surprisingly, the molar mass values of copolymers prepared with **3-MAO** are low and M_w/M_n of the copolymer obtained with **3-MAO** with lowest yield is broader. The plot of molar masses (M_n) versus the ratio [N]/[P] in feed is displayed in Chart 5. The changes in M_n values of copolymers synthesized by the two catalytic systems by increasing [N]/[P] ratios in the feed are opposite: indeed, whereas in the series obtained with *rac*-Et(Ind)$_2$ZrCl$_2$, the M_n values increase with norbornene in the feed and in the copolymer, in the series prepared with *rac*-Me$_2$Si(2-Me-Ind)$_2$ZrCl$_2$ the M_n values decrease, probably because the copolymerization reaction becomes so slow that the chain transfers are more probable.

The thermal properties of copolymers have been investigated by DSC (Table 1). T_g values of copolymers from **3-MAO** are much lower than those from **1-MAO**. A comparison between samples obtained in similar conditions reveals a difference of ~80 °C in T_g values, 22.2 °C with **3-MAO** at [N]/[P] = 0.29, and 104 °C with **1-MAO** at [N]/[P] = 0.22. Differences in molar masses may also contribute to lower T_g values of copolymers prepared with **3-MAO**. The evolution of T_g values versus f_N in the copolymers are plotted in Chart 6. Inspection of the Chart reveals that the differences in T_g values arise, mainly, from the different amount of norbornene incorporated in the copolymer.

Chart 5. Plot of M_n Values for P−N Copolymers Obtained with *rac*-Et(Ind)$_2$ZrCl$_2$ and *rac*-Me$_2$Si(2-Me-Ind)$_2$ZrCl$_2$ at 5 bar, 40 °C versus [N]/[P] in the Feed

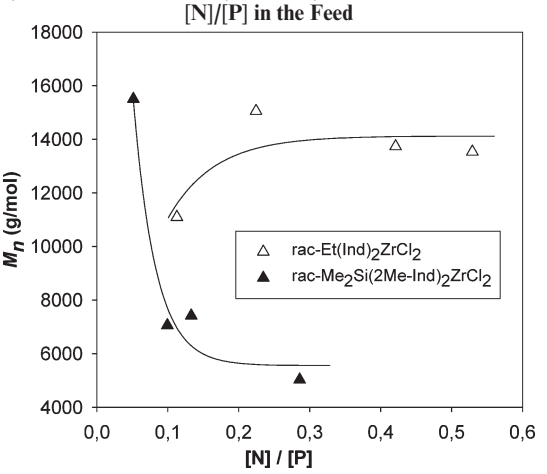

Chart 6. Plot of T_g Values for P−N Copolymers Obtained with *rac*-Et(Ind)$_2$ZrCl$_2$ and *rac*-Me$_2$Si(2-Me-Ind)$_2$ZrCl$_2$ at 5 bar, 40 °C versus f_N in the Copolymers

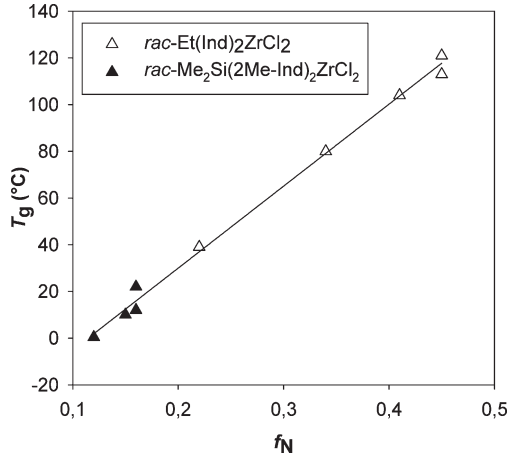

NMR Investigation on Propene−Norbornene Copolymers and Determination of Reactivity Ratios. *Microstructure at Triad Level.* Microstructure of P−N copolymers is very complicated. Propene, P, may be present in the copolymer chain in the forms P_{12}, P_{13}, and P_{21}, as in the copolymer chain of a random P−N copolymer sketched in Chart 2, where differences in tacticity are ignored. Because of the asymmetry of the bonds between N and P_{12} (or P_{21}), in general, two diads M_1M_2 and M_2M_1 are not equivalent. The same holds for triads, and thus 23 triads are possible when assuming that units P_{13} and P_{21} may be inserted only after N. In our denomination, each triad $M_1M_2M_3$ is depicted as $M_3M_2M_1$, that is, running from right to left (the catalyst metal ideally being bound to the extreme left side of the chain).

^{13}C NMR is one of the most powerful tools for microstructural analysis and for elucidation of important details of the polymerization mechanism. Therefore, the P−N copolymers have been analyzed by ^{13}C NMR spectroscopy. In Figure 1, two ^{13}C NMR spectra of samples with similar [N]/[P] ratios produced with **1-MAO** and **3-MAO** catalysts are compared. Some differences in the two spectra can be observed.

A first diversity is the appearance of groups of signals at about 15.54, 16.22, and 16.34 ppm (CH_3 from DEPT), which have been assigned to the methyl carbon atom of central monomer in $P_{21}P_{12}P_{12}$, $P_{21}P_{12}N$, and $NP_{21}P_{12}$, respectively. An unexpected significant difference is in the region of CH_3 signals ranging from 17.80 to 19.83, which gives information on the microstructure of PP blocks; inspection of the signals of this region reveals that the PP blocks of the copolymers obtained with *rac*-Me_2Si(2-Me-Ind)$_2ZrCl_2$ are not as highly isotactic as one would expect. (See below for further details.) Indeed, it is well known that the methyl group in position 2 of *rac*-Me_2Si(2-Me-Ind)$_2ZrCl_2$ imparts much higher stereoregularity to polypropene homopolymers than *rac*-Et(Ind)$_2$-$ZrCl_2$.

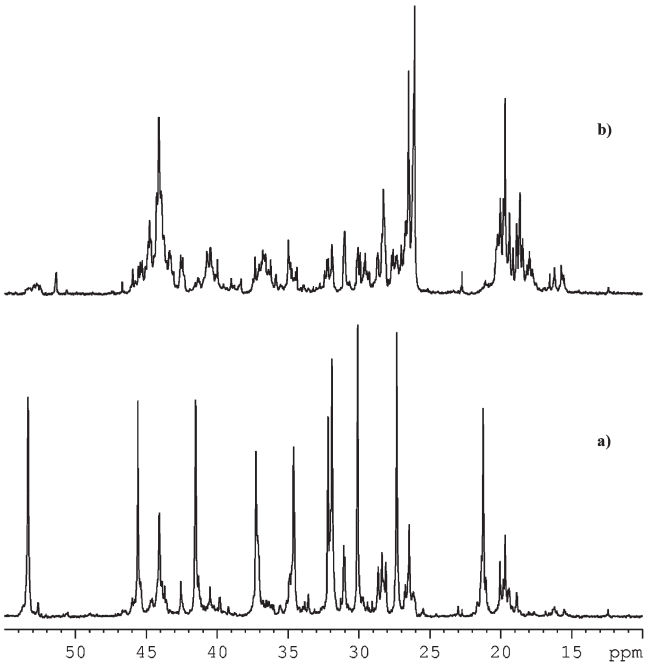

Figure 1. ^{13}C NMR spectra of P−N copolymers prepared with (a) *rac*-Et(Ind)$_2ZrCl_2$ (**1**) ([N]/[P]$_{feed}$ = 0.11, f_N = 0.34) and (b) *rac*-Me_2Si(2-Me-Ind)$_2ZrCl_2$ (**3**) ([N]/[P]$_{feed}$ = 0.10, f_N = 0.16).

The complexity of these spectra prompted us to a thorough study of the spectra of a number of P−N copolymers prepared with catalysts **1-MAO** and **3-MAO**. The analysis, the object of the reference 18, was based on the comparison of ^{13}C NMR spectra of P−N copolymers of various composition, 2D NMR techniques, including homonuclear $^1H-^1H$ and heteronuclear $^1H-^{13}C$ experiments, and a methodology for the quantitative analysis of copolymer sequences. This led to new assignments and the ability to quantify the copolymer microstructure at triad level. The most significant triad molar fractions estimated for the two series of copolymers are collected in Table 2. The analysis of this work did not provide a complete description at triad level; however, it was possible to obtain the molar fractions of all possible diads, which are collected in Table 3.

The greatest differences between the triad distributions of the two series are in the high value of triad $NP_{12}N$ in the alternating copolymer from **1-MAO** in contrast with the vanishingly low content of this triad in the samples from **3-MAO** and in the persistently high content of $P_{12}P_{12}P_{12}$, even at high feed ratio in the same series. In contrast, $NP_{12}P_{12}$ is quite similar for the two series of copolymers. These features clearly point out the difficulty of this catalyst to insert a norbornene into a Mt-$P_{12}N$ bond, indicating the importance of the penultimate inserted monomer. A most interesting difference is in the amount of triads containing propene misinsertions or regioerrors, which is greater in the series from **3-MAO** than from **1-MAO**. This is unexpected because in P homopolymerization, the two catalysts have opposite behaviors.

It is worth noting the relevant amount of $NP_{13}P_{12}$ and $NP_{13}N$ and thus of 1,3-enchained units, which arise when a propene is inserted into a Mt-N bond. In particular, the value of $NP_{13}P_{12}$ is quite high in the series from **3-MAO**, whereas that of $NP_{13}N$ is higher in the series from **1-MAO**. Interestingly, for catalyst **3-MAO**, the molar fraction of $NP_{12}P_{12}$ is similar or even lower than the molar fractions of $NP_{13}P_{12}$

Table 2. Triads Molar Fractions of P−N Copolymers Obtained by Catalysts 1 and 3 at Different [N]/[P] Feed Ratio[a]

cat.	entry	[N]/[P]	f_N	$P_{12}P_{12}P_{12}$	$P_{12}P_{12}N$	$NP_{12}P_{12}$	$NP_{12}N$	$P_{13}P_{12}P_{12}$	$P_{13}P_{12}N$	$P_{21}P_{12}P_{12}$	NNP_{12}	$P_{21}P_{12}N$	$NP_{13}P_{12}$	$NP_{13}N$	$NP_{21}P_{12}$
				*T*1[b]	*T*2	*T*3	*T*4	*T*5	*T*6	*T*7	*T*13	*T*8	*T*21	*T*22	*T*23
1	8	0.11	0.34	0.226	0.069	0.058	0.222	0.000	0.017	0.012	0.004	0.006	0.017	0.017	0.018
1	9	0.22	0.41	0.129	0.050	0.035	0.260	0.006	0.025	0.009	0.013	0.006	0.031	0.025	0.015
1	10	0.42	0.45	0.086	0.043	0.026	0.298	0.011	0.004	0.007	0.019	0.005	0.014	0.047	0.012
1	11	0.53	0.45	0.103	0.039	0.015	0.286	0.017	0.001	0.007	/	0.005	0.018	0.052	0.012
3	2	0.05	0.12	0.635	0.061	0.029	0.000	0.000	0.039	0.032	0.000	0.005	0.039	0.000	0.037
3	3	0.10	0.16	0.537	0.085	0.034	0.006	0.018	0.031	0.032	0.000	0.006	0.049	0.006	0.038
3	4	0.13	0.15	0.564	0.068	0.029	0.025	0.008	0.036	0.031	0.000	0.006	0.044	0.002	0.037
3	5	0.29	0.16	0.513	0.103	0.051	0.000	0.043	0.035	0.009	0.000	0.002	0.078	0.001	0.010

[a] Calculated with the procedure reported in reference 18 [b] Triad denomination as in reference 18.

Table 3. Diads Molar Fractions of P−N Copolymers Obtained by Catalysts 1 and 3 at Different [N]/[P] Feed Ratio Calculated from Triads Molar Fractions of Table 2

cat.	entry	f_N	[N]/[P]	($P_{12}P_{12}$)	($P_{12}N$)	(NP_{12})	(NP_{13})	(NP_{21}) = ($P_{21}P_{12}$)	($P_{13}P_{12}$)	($P_{13}N$)	(NN)
1	8	0.34	0.11	0.295	0.314	0.280	0.034	0.018	0.017	0.017	0.008
1	9	0.41	0.22	0.179	0.342	0.295	0.056	0.015	0.031	0.025	0.041
1	10	0.45	0.42	0.129	0.350	0.325	0.062	0.012	0.014	0.047	0.049
1	11	0.45	0.53	0.142	0.332	0.312	0.061	0.012	0.018	0.052	0.061
3	2	0.12	0.05	0.696	0.104	0.029	0.039	0.037	0.039	0.000	0.020
3	3	0.16	0.10	0.621	0.128	0.040	0.056	0.038	0.049	0.006	0.023
3	4	0.15	0.13	0.632	0.134	0.054	0.046	0.037	0.044	0.002	0.014
3	5	0.16	0.29	0.615	0.139	0.051	0.079	0.010	0.078	0.001	0.015

and $NP_{21}P_{12}$ (except for the sample obtained at [N]/[P] = 0.29), which means that the 1,2 propene insertion after N is so difficult that the 1,3 insertion is preferred. In addition, $NP_{21}P_{12}$ is almost independent from [N]/[P] ratio in the feed, except for the sample obtained at the highest N concentration, where the $NP_{21}P_{12}$ molar fraction is the lowest. Moreover, in the series from **3-MAO**, the molar fraction of $NP_{13}N$ is also lower than that of $NP_{13}P_{12}$, again an indication that for catalyst **3-MAO**, penultimate effects are very important.

Determination of Reactivity Ratios. We shall now try to express the above results on triad composition of the P−N chain (and related considerations on penultimate effects) in terms of reactivity ratios. When the insertion of a comonomer is influenced by the last inserted unit (ultimate effect) or by the penultimate unit, the first order or the second Markovian statistical model, respectively, is adopted to determine the reactivity ratios.[19−23] Our studies on E−N copolymerizations have shown that when hindered monomers such as norbornene are involved, second-order models are needed to describe the copolymerization also with metallocene catalysts.[24] However, the second Markovian statistical model needs detailed information on the copolymer microstructure at least at triad level. This motivated our elucidation of spectra of P−N copolymers. Triad molar fractions suggest that P−N copolymerization with **3-MAO** are dominated by ultimate and penultimate effects. We have first used the calculated diads of Table 3 to evaluate the reactivity ratios r_i. Although the present work does not provide the molar fractions of all the possible triads, it is also possible to evaluate interesting r_{ij}[19] that give information not present in r_i.

In the following, well-known general equations of copolymerization statistics[19] are applied to the specific case of P−N copolymers at diad and triad level. Details of the determination of the copolymerization parameters are given in the Supporting Information.

In the present case, we have to consider four comonomers. Here indexes 1 and 2 indicate 1,2-inserted propene units (P_{12}) and norbornene (N), respectively, whereas we denominate as 3 and 4 1,3- and 2,1-inserted propene units (P_{13} and P_{21}), respectively. If we assume ultimate effects only, then the first-order Markov is sufficient and the copolymerization parameters, r_i, are defined and related to the probabilities P (P_{lm} is the probability that monomer, m, is inserted in a bond *l-Metal*) by equations

$$r_1 = k_{11}/k_{12} = (1/P_{12} - 1)f,$$

$$r_2 = k_{22}/k_{21} = (1/P_{21} - 1)/f$$

where f is the monomer feed ratio [2]/[1].

In the case of P−N copolymers, we have to consider all possible rate constants

$$k_{11}\ k_{12} \quad k_{21}\ k_{22}\ k_{23}\ k_{24} \quad k_{31}\ k_{32}$$

and to define the reactivity ratios

$$r_1 = k_{11}/k_{12} = k_{\mathrm{P12P12}}/k_{\mathrm{P12N}} \quad r_2 = k_{22}/k_{21} = k_{\mathrm{NN}}/k_{\mathrm{NP12}}$$

$$r_2' = k_{22}/k_{23} = k_{\mathrm{NN}}/k_{\mathrm{NP13}} \quad r_2'' = k_{22}/k_{24} = k_{\mathrm{NN}}/k_{\mathrm{NP21}}$$

$$r_3 = k_{31}/k_{32} = k_{\mathrm{P13P12}}/k_{\mathrm{P13N}}$$

It may be easily shown that

$$r_1 = (P_{12}P_{12})f/(P_{12}N) \quad r_3 = (P_{13}P_{12})f/(P_{13}N)$$

$$r_2 = (NN)/[(NP_{12})f], \quad r_2' = (NN)/[(NP_{13})f]$$

$$r_2'' = (NN)/[(NP_{21})f]$$

When the insertion of a comonomer is influenced by the penultimate unit, the second-order Markov model is needed, and the copolymerization parameters r_{ij} are defined and related to the probabilities P, (Here P_{lmn} is the probability that monomer n is inserted in a bond *lm-Metal*.)

Experimental tetrad molar fractions are needed to best fit the probabilities P, with second-order Markov model. When only triads are available, it is possible to evaluate copolymerization parameters r_{ij}. In the present case, we have to consider all possible rate constants of the four different comonomers

$$k_{111}\ k_{112} \quad k_{211}\ k_{212} \quad k_{311}\ k_{312} \quad k_{411}\ k_{412}$$

$$k_{121}\ k_{122}\ k_{123}\ k_{124} \quad k_{221}\ (k_{222} = 0)\ k_{223}\ k_{224}$$

$$k_{321}\ k_{322}\ k_{323}\ k_{324}$$

$$k_{231}\ k_{232}$$

and to define the reactivity ratios

$$r_{11} = k_{111}/k_{112} = k_{\mathrm{P12P12P12}}/k_{\mathrm{P12P12N}}$$
$$r_{21} = k_{211}/k_{212} = k_{\mathrm{NP12P12}}/k_{\mathrm{NP12N}}$$
$$r_{31} = k_{311}/k_{312} = k_{\mathrm{P13P12P12}}/k_{\mathrm{P13P12N}}$$
$$r_{41} = k_{411}/k_{412} = k_{\mathrm{P21P12P12}}/k_{\mathrm{P21P12N}}$$
$$r_{23} = k_{231}/k_{232} = k_{\mathrm{NP13P12}}/k_{\mathrm{NP13N}}$$
$$r_{12} = k_{122}/k_{121} = k_{\mathrm{P12NN}}/k_{\mathrm{P12NP12}}$$
$$r_{12}' = k_{122}/k_{123} = k_{\mathrm{P12NN}}/k_{\mathrm{P12NP13}}$$
$$r_{12}'' = k_{122}/k_{124} = k_{\mathrm{P12NN}}/k_{\mathrm{P12NP21}}$$
$$r_{22} = k_{222}/k_{221} = 0$$
$$r_{22}' = k_{223}/k_{221} = k_{\mathrm{NNP13}}/k_{\mathrm{NNP12}}$$
$$r_{22}'' = k_{224}/k_{221} = k_{\mathrm{NNP21}}/k_{\mathrm{NNP12}}$$
$$r_{32} = k_{322}/k_{321} = k_{\mathrm{P13NN}}/k_{\mathrm{P13NP12}}$$
$$r_{32}' = k_{322}/k_{323} = k_{\mathrm{P13NN}}/k_{\mathrm{P13NP13}}$$
$$r_{32}'' = k_{322}/k_{324} = k_{\mathrm{P13NN}}/k_{\mathrm{P13NP21}}$$

We can derive some of the reactivity ratios from the following relationships (holding under steady state conditions)

$$r_{11} = (\mathrm{P_{12}P_{12}P_{12}})f/(\mathrm{P_{12}P_{12}N})$$

$$r_{21} = (\mathrm{NP_{12}P_{12}})f/(\mathrm{NP_{12}N})$$

$$r_{31} = (\mathrm{P_{13}P_{12}P_{12}})f/(\mathrm{P_{13}P_{12}N})$$

$$r_{41} = (\mathrm{P_{21}P_{12}P_{12}})f/(\mathrm{P_{21}P_{12}N})$$

$$r_{23} = (\mathrm{NP_{13}P_{12}})f/(\mathrm{NP_{13}N})$$

Because not all triad molar fractions have been determined, we might obtain r_{22}' and r_{22}'' as a sum, whereas it

Table 4. Reactivity Ratios Calculated from Diads Molar Fractions of Table 3

cat.	entry	[N]/[P]	r_1 (k_{P12P12}/k_{P12N})	r_3 (k_{P13P12}/k_{P13N})	r_2 (k_{NN}/k_{NP12})	$r_{2'}$ (k_{NN}/k_{NP13})	$r_{2''}$ (k_{NN}/k_{NP21})
1	8	0.11	0.10	0.11	0.26	2.14	4.04
1	9	0.22	0.12	0.27	0.63	3.33	12.42
1	10	0.42	0.15	0.13	0.36	1.88	9.72
1	11	0.53	0.23	0.18	0.37	1.89	9.59
3	2	0.05	0.33	> 10	13.79	10.26	10.81
3	3	0.10	0.49	0.82	5.75	4.11	6.05
3	4	0.13	0.61	2.86	1.99	2.34	2.91
3	5	0.29	1.28	22.62	1.01	0.65	5.17

Table 5. Reactivity Ratios Calculated from Triads Molar Fractions of Table 2

cat.	entry	f_N	[N]/[P]	r_{11} ($k_{P12P12P12}/k_{P12P12N}$)	r_{21} ($k_{NP12P12}/k_{NP12N}$)	r_{31} ($k_{P13P12P12}/k_{P13P12N}$)	r_{41} ($k_{P21P12P12}/k_{P21P12N}$)	r_{23} ($k_{NP13P12}/k_{NP13N}$)
1	8	0.34	0.11	0.36	0.03	0.00	0.22	0.11
1	9	0.41	0.22	0.57	0.03	0.05	0.33	0.27
1	10	0.45	0.42	0.84	0.04	1.16	0.59	0.13
1	11	0.45	0.53	1.40	0.03	9.00	0.74	0.18
3	2	0.12	0.05	0.52	> 10		0.32	
3	3	0.16	0.10	0.63	0.57	0.06	0.53	0.82
3	4	0.15	0.13	1.08	0.15	0.03	0.67	2.88
3	5	0.16	0.29	1.44	> 10	0.36	1.31	22.62

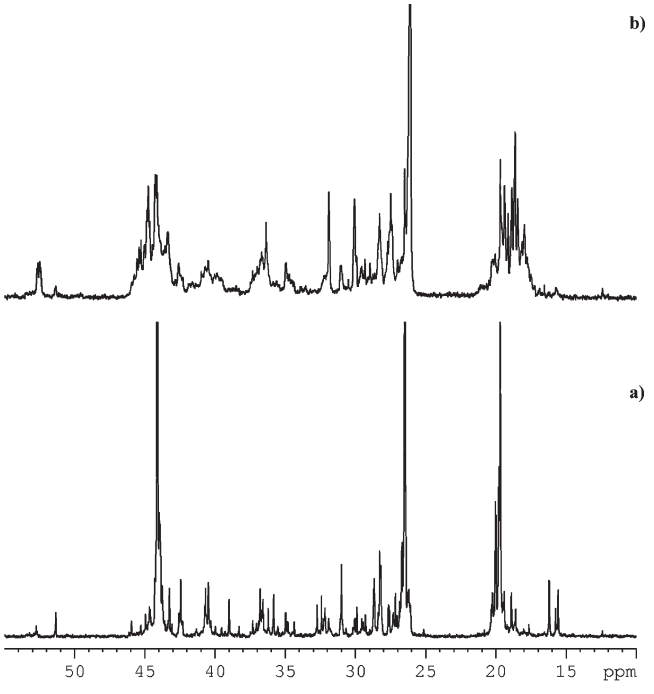

Figure 2. ^{13}C NMR spectra of P−N copolymers produced with *rac*-$Me_2Si(2\text{-Me-Ind})_2ZrCl_2$ at 5 bar, 40 °C: (a) [N]/[P] = 0.05 and f_N = 0.12; (b) [N]/[P] = 0.29 and f_N = 0.15.

would be even more complicated to derive r_{12}, r_{12}', and r_{22}''. Also considering the errors present in some of the minor molar fractions involved, at present, we omit such calculations.

The r_i values calculated from diads and those r_{ij} calculated from triads of P−N copolymers prepared with **1-MAO** and **3-MAO** are collected in Tables 4 and 5, respectively.

The trends offered by parameters r_i and r_{ij} are significant. The r_1 (= k_{P12P12}/k_{P12N}) and r_3 (= k_{P13P12}/k_{P13N}) values for **1-MAO** are similar and are close to zero, indicating the

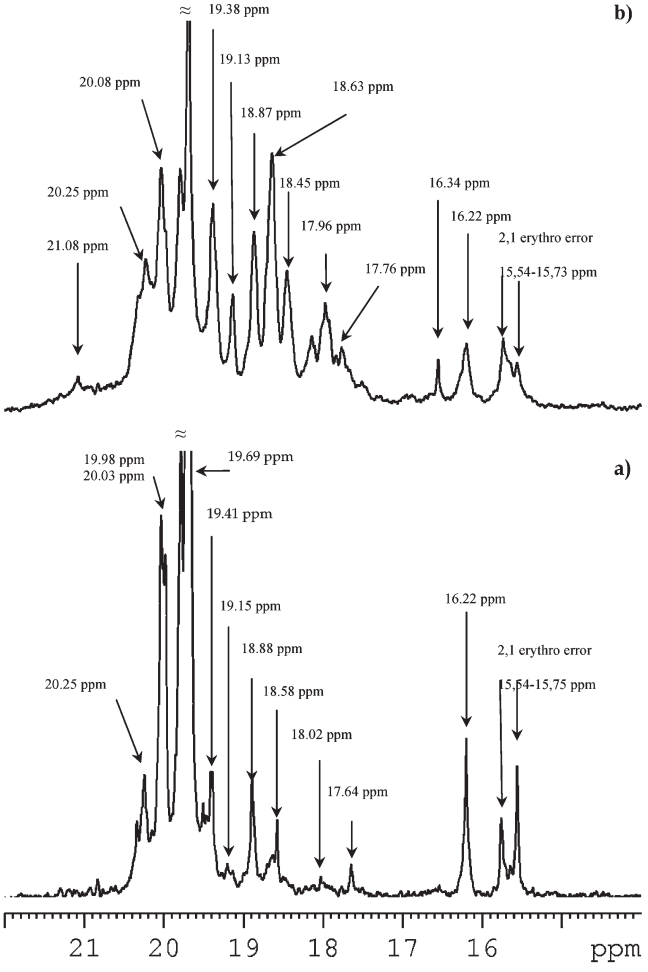

Figure 3. Methyl region of ^{13}C NMR spectra of P−N copolymers produced with *rac*-$Me_2Si(2\text{-Me-Ind})_2ZrCl_2$ at 5 bar, 40 °C: a) [N]/[P] = 0.05 and f_N = 0.12; b) [N]/[P] = 0.13 and f_N = 0.15. Assignments of peaks at pentad level.

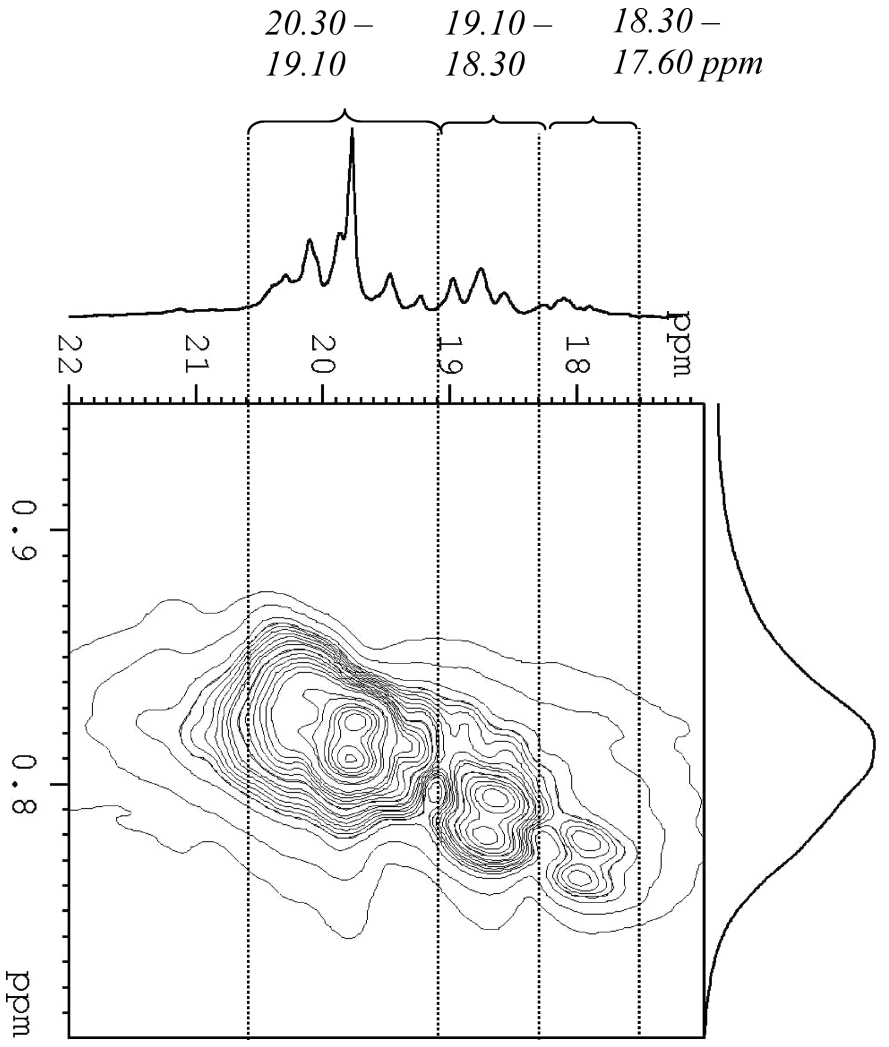

Figure 4. Expansion of methyl region of the gHSQC experiment of a P−N copolymer obtained with catalyst **3** ([N]/[P] = 0.13, f_N = 0.15).

tendency to alternate P_{12} or P_{13} and N (Table 4). The r_2 values are also low, below 0.5, but higher than r_1. The r_2 (= k_{NN}/k_{NP12}), $r_{2'}$ (= k_{NN}/k_{NP13}), and $r_{2''}$ (= k_{NN}/k_{NP21}) values highlight the differences in the facilities of P_{12}, P_{13} and P_{21} insertions in the Mt−N bond. The $r_{2''}$ values higher than $r_{2'}$ confirm the tendency of 2,1 propene insertion to isomerize to 1,3. The r_1 values for **3-MAO** are greater than those for **1-MAO**; this is certainly related to the higher activity in propene homopolymerization and thus to a higher k_P of **3-MAO**. We recall that for catalyst **3-MAO** we obtain copolymers with a maximum N content of ~16 mol %, but at low N concentration in the feed, the N content in the copolymer is still greater than in E−N copolymerization. Therefore, also for this catalyst, norbornene insertions compete with propene insertions but less than for **1-MAO**. Indeed, r_2 values for **3-MAO**, greater than for **1-MAO**, are higher than r_1 values; this is in contrast with E−N copolymerizations, and it is certainly related to the difficulty to insert P after N. Moreover, the r_2, $r_{2'}$, and $r_{2''}$ values are quite similar in copolymers from **3-MAO**, indicating that the last N inserted unit slows down P_{12} insertions so that all possible forms of P insertions (P_{12}, P_{13}, and P_{21}) have a similar probability of insertion.

More detailed information can be gained from the results of r_{ij} values (Table 5). Regarding the r_{11} (= $k_{P12P12P12}/k_{P12P12N}$), r_{31} (= $k_{P13P12P12}/k_{P13P12N}$), and r_{41} (= $k_{P21P12P12}/k_{P21P12N}$) values, all increase with N concentration in the feed. The r_{41} values are quite similar to r_{11} for each catalyst, and both r_{11} and r_{41} values reach values with both catalysts; of course, those from catalyst **3-MAO** are much higher than those from **1-MAO** at parity of feed ratio. More interesting are the r_{21} (= $k_{NP12P12}/k_{NP12N}$) and r_{23} (= $k_{NP13P12}/k_{NP13N}$) values. The r_{21} values are close to 0 for copolymers with **1-MAO**, whereas those of copolymers with **3-MAO** are higher, although affected by errors. This again indicates the tendency to give alternating and random copolymers of these two catalysts. This difference is more evident when comparing the r_{23} values. Therefore, the high r_{23} values indicate that **3-MAO** does not allow an N insertion even into a Mt-P_{13}N bond, demonstrating a penultimate effect.

*Tacticity of PP Blocks of P−N Copolymers Obtained with Catalyst **3-MAO***. In Figure 2, two examples of ^{13}C NMR spectra of P−N copolymers obtained with catalyst **3-MAO**, with low and high [N]/[P] ratios, are reported. Even though the content of norbornene in the copolymer is rather similar, the spectra are clearly very different.

Figure 3 shows the expansions of the methyl region of two ^{13}C NMR spectra of P−N copolymers obtained at low and high [N]/[P]. The two spectra clearly reveal a great difference in the tacticity of the PP blocks.

The correct assignment of methyl region reported in Figure 3 has been confirmed at the triad level on the basis of the gHSQC (gradient-assisted heteronuclear single quantum coherence) experiment in Figure 4. Figure 4 is rotated

90° with respect to the conventional representation to compare Figure 3 with the correspondent portion of gHSQC. Observing the Figure, showing resonances correlating ^{13}C and ^{1}H atoms directly bonded, the reader can immediately visualize a grouping of methyl signals in three areas that correspond to *mm*, *mr*, and *rr*-centered methyls, as reported in literature.[25] We have attributed the signals between 19.10 and 21 ppm to the *mm* triad, the signals between 18.30 and 19.15 ppm to the *mr* triad, and those between 17.60 and 18.30 ppm to the *rr* triad.

We have quantified the tacticity at triad level to evaluate the effect of [N]/[P] feed ratio on the microstructure of PP blocks. The correlation between molar fractions of tactic triads with [N]/[P] in the feed of P−N copolymers produced with **3-MAO** is reported in Chart 7.

The Chart clearly visualizes that in the copolymers prepared with the *rac*-$Me_2Si(2\text{-Me-Ind})_2ZrCl_2$ system; by increasing the norbornene content in the feed, the *mm* triad molar fraction decreases, whereas the fraction of the *rr* triad increases. A similar but much smaller effect is observed in copolymers prepared with *rac*-$Et(Ind)_2ZrCl_2$, the other C_2 symmetric catalyst investigated. The strong effect observed with **3-MAO** must be related to isomerization reactions, which cause a change in the chirality of the last inserted propene.

Isospecific C_2 symmetric catalysts displayed a decrease in isotacticity of PP samples, when polymerization were carried out at low propene concentrations. Interesting studies, including isotopically labeled propene, were performed to study the mechanism originating this phenomenon. Evidences support the chain epimerization as the most plausible mechanism.[26,27] It seems that at high norbornene concentration in the feed, with this catalyst, which has difficulty in accommodating a norbornene into Mt-P_{12}N (and perhaps even into Mt-$P_{12}P_{12}$N because the N content into the copolymer does not exceed 16 mol %), this unimolecular isomerization event, whatever the mechanism, becomes probable.

Chart 7. Molar Fractions of Tactic Triads of PP Blocks in P−N Copolymers Produced with *rac*-$Me_2Si(2\text{-Me-Ind})_2ZrCl_2$ with Increasing [N]/[P] in the Feed

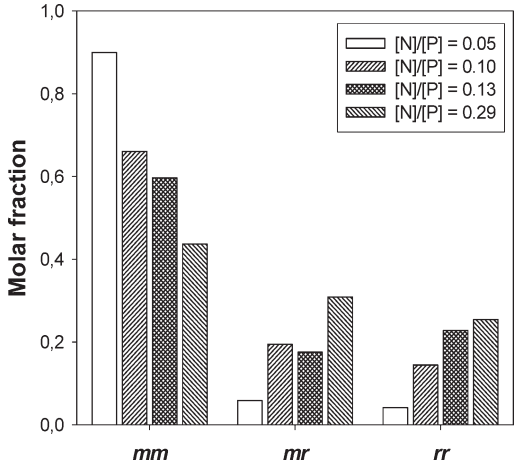

^{1}H NMR of P−N Copolymers and Chain Terminations. Analysis of the end groups by ^{13}C and ^{1}H NMR spectra of polymers gives important information on the reactions involved in chain transfers and terminations. Scheme 1 summarizes the processes that could lead to the formation of the regioirregularities and to the most interesting left end groups. Because it was demonstrated that chain transfers after an inserted norbornene unit are difficult, only the microstructures that derive from primary and secondary

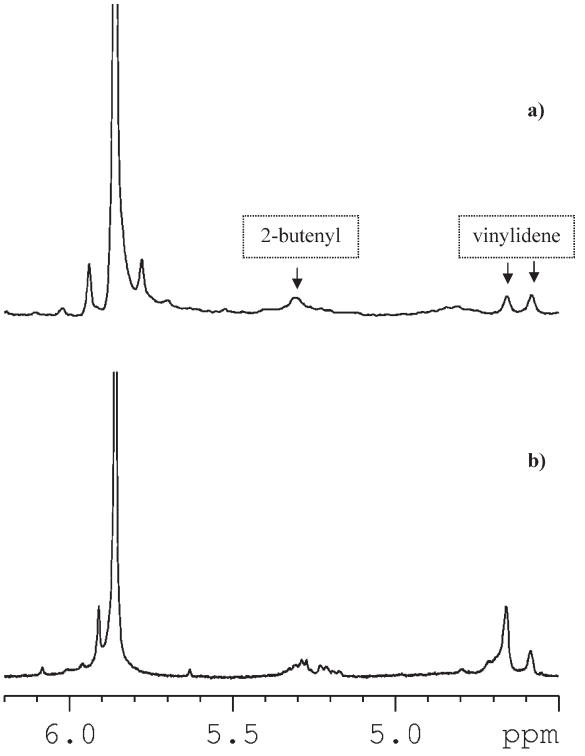

Figure 5. 2-Butenyl and vinylidene end groups signals in ^{1}H NMR spectra of P−N copolymers produced with *rac*-$Me_2Si(2\text{-Me-Ind})_2ZrCl_2$ at 5 bar, 40°; (a) [N]/[P] = 0.10 and f_N = 0.16; (b) [N]/[P] = 0.13 and f_N = 0.15.

Scheme 1. Processes Involved in the Formation of the Most Interesting Left End Groups

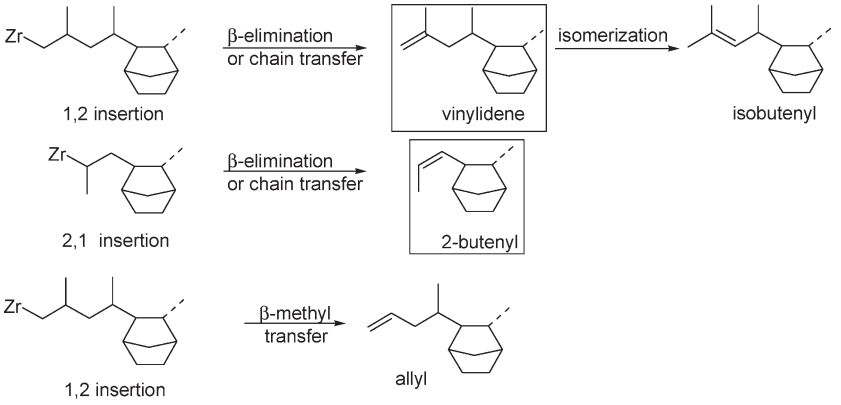

Table 6. Molar Fractions of 2-Butenyl and Vinylidene End Groups Obtained by the Analysis of ^{1}H NMR Spectra of P−N Copolymers

catalyst	entry	[N]/[P] feed	f_N	$M_n \times 10^{-3}$ (g/mol)	f(vinyl) $\times 10^3$	f(2-butenyl) $\times 10^3$
3	2	0.05	0.12	15.5	0.59	0.13
3	3	0.10	0.16	7.1	1.88	1.03
3	4	0.13	0.15	7.4	0.83	0.08
3	5	0.29	0.16	5.0	3.96	5.61
1	7	0.06	0.22	4.0	1.14	4.71
1	8	0.11	0.34	11.1	0.80	3.17
1	9	0.22	0.41	15.1	0.62	2.70
1	10	0.42	0.45	13.7	0.00	2.03
1	11	0.53	0.45	13.5	0.29	2.00

Scheme 2. 2,1 and 1,3 Insertions and Chain Epimerization Occurring with Catalyst 3

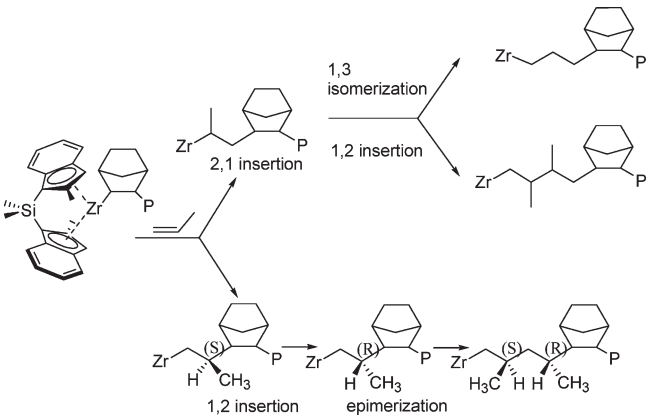

propene insertions, respectively, are shown. The molar fractions of 2-butenyl and vinylidene end groups, based on the analysis of the integrated signals due to the ^{1}H NMR spectra of the polymers (Figure 5), are reported in Table 6. In general, we observe a greater amount of 2-butenyl end groups arising from termination at a Mt-P_{21} than of vinylidene arising from termination at a Mt-P_{12}. This is opposite to what was observed in P homopolymerization with **1-MAO** and **2-MAO**.[16] Moreover, the amount of 2-butenyl end groups is greater for the samples with lower molar fractions of triads containing the P_{21} unit. Therefore, 2-butenyl end groups are greater for samples obtained with **1-MAO** than with **3-MAO**, except for the sample obtained at the highest norbornene concentration in feed with **3-MAO**, that is, the one in which we observed the lowest molar fractions of triads containing P_{21} units. This is additional evidence that the limiting step in P−N copolymerization is the difficulty to insert a propene after N, which causes 2,1 insertions with subsequent isomerization to 1,3 propene insertions as well as chain epimerization.

Thus, 2-methyl substitution of the indenyl ligand of **3** makes the insertion of N into the Mt-P_{12}N bond so difficult that *R*-*S* isomerization of the last inserted propene unit is possible, at relatively high [N]/[P] ratios, i.e. in starved propene conditions. Moreover, with this catalyst, which does not tend to give chain transfers to the monomer in P homopolymerization, a $P_{2,1}$ insertion can compete with a $P_{1,2}$ insertion: as a consequence the molar fractions of triads containing $P_{2,1}$ are relatively high, while with catalyst **1-MAO** the $P_{2,1}$ insertions tend to terminate giving more 2-butenyl chain end groups. The isomerization to 1,3 insertions is similar in the copolymers prepared with both catalysts (Scheme 2).

Conclusions

The copolymerization of propene and norbornene by catalytic systems composed of **3-MAO** was investigated and compared with that by **1-MAO**. Methyl 2 substitution on the indenyl ligand in **3** has an unexpected and strong influence on the catalyst behavior in P−N copolymerization, causing a strong decrease in catalytic activity, molar fractions, f_N, T_g, and M_n values. P−N copolymers with maximum 16 mol % of norbornene were obtained by **3-MAO** in contrast with those highly alternating obtained by **1-MAO**. The microstructural analysis by ^{13}C NMR of the copolymers at triad level and the reactivity ratios r_i and r_{ij} obtained from diads and triads, respectively, give evidence of the tendency to alternate or not to alternate P and N comonomers and information on the probability of insertion of N and of the possible forms of P insertion (P_{12}, P_{13}, and P_{21}) and on penultimate effects.

The highly alternating nature of the copolymerization with **1-MAO** is evidenced by the high value of $NP_{12}N$ triads and from the low r_1 and r_3 values as well as from the low r_{21} and r_{23} values, all close to zero.

The difficulty of catalyst **3-MAO** to insert a norbornene into a Mt-P_{12}N bond appears from the vanishingly low content of $NP_{12}N$ triads and from the r_1 values greater than those for **1-MAO** but lower than in E−N copolymerizations. Therefore, for this catalyst, norbornene insertions also compete with propene insertions but less than for **1-MAO**. The higher r_{11} and r_{21} values for **3-MAO** with respect to **1-MAO** are a clear indication of the different tendency to give alternating or random copolymers of the two catalysts. The r_2 values for **3-MAO**, greater than for **1-MAO**, and higher than r_1 values testify the difficulty to insert P after N.

An interesting information regards the unexpected amount of triads containing propene misinsertions or regioerrors, which are greater in the series from **3-MAO** than from **1-MAO**. Regarding 1,3-enchained units, it is worth noting the relevant amount of $NP_{13}P_{12}$ in the series from **3-MAO** and of $NP_{13}N$ in the series from **1-MAO**, again reflecting the different tendency to alternate the comonomers of the two catalysts and the important penultimate effects with **3-MAO**. The $r_{2''}$ values higher than $r_{2'}$ confirm the tendency of 2,1 propene insertion to isomerize to 1,3, especially in P−N copolymerizations with **1-MAO**.

Interestingly, the r_2, $r_{2'}$, and $r_{2''}$ values quite similar in copolymers from **3-MAO** show that the last N inserted unit slows down P_{12} insertions so that all possible forms of P insertions (P_{12}, P_{13}, and P_{21}) have similar probability of insertion. The high r_{23} values indicate that **3-MAO** does not allow an N insertion, even into a Mt-P_{13}N bond demonstrating a penultimate effect.

Assignments of tactic triads allowed to quantify the great decrease in the tacticity of the PP blocks in the copolymers prepared with **3-MAO** with increasing the norbornene content in the feed. With this catalyst, which has difficulty in accommodating a norbornene into Mt-P_{12}N, probable unimolecular epimerization events become probable.

Chain end groups analysis revealed a greater amount of 2-butenyl end groups arising from termination at a Mt-P_{21} than of vinylidene arising from termination at a Mt-P_{12}. The greater amount of 2-butenyl end groups in samples with lower molar

fractions of triads containing the P_{21} unit and for samples obtained with **1-MAO** gives an evidence that the limiting step in P−N copolymerization is the difficulty to insert a propene after N, which causes 2,1 insertions with subsequent isomerization to 1,3 propene insertions as well as chain epimerization under starved propene conditions with **3-MAO**.

Experimental Part

General Conditions. All experiments were performed under dry nitrogen, in glovebox or by using standard Schlenk line techniques. MAO (10 wt % as toluene solution, Crompton) was dried (50 °C, 3 h, 0.1 mmHg) before use. Toluene was dried and distilled from sodium. *rac*-$Me_2Si(2\text{-Me-Ind})_2ZrCl_2$was purchased from Boulder. Nitrogen and propene gases were purified by passage over columns of $CaCl_2$, molecular sieves, and BTS catalysts. Norbornene was distilled from sodium and used as stock solution in toluene.

Polymerization. Experiments were performed in a Buchi BEP2000 autoclave with 1 L reactor. Before starting with the polymerization, the reactor was conditioned by means of three N_2/vacuum cycles performed at 70 °C; then, in a typical experiment, the reactor was charged with a solution of 26 mmol of cocatalyst (dried MAO + Al^iBu_3 (ratio 3.3)) and an opportune quantity of norbornene (used as toluene solution) with ∼300 mL of dried toluene. After thermal equilibration of the reactor system at 40 °C, propene was continuously added until saturation (at a pressure of 5 bar). About 1 h after the equilibrium was reached, the 25 mL injector was charged with 10 mL of a solution of 10 μmol of catalyst in toluene, typically [Zr] = 0.010 mmol·L^{-1}, Al/Zr = 2000). The injector with the catalyst solution was pressurized to the proper pressure, higher than that present inside the reactor, and the solution was injected into the reactor. The mixture was stirred for a variable time period (between 5 min and 3 h) depending on the catalytic activity and the norbornene content in feed. The reaction was then terminated by the addition of a small amount of acidic ethanol; the polymer was precipitated upon pouring the whole reaction mixture in ethanol (1 L) to which concentrated HCl (10 mL) had been added. The product was at last collected by filtration, washed again with ethanol, and finally dried under vacuum at 70 °C.

Propene concentration in toluene was calculated according to Henry's law, as already described.[5d]

^{13}C NMR. For ^{13}C NMR, ∼100 mg of copolymer was dissolved in $C_2D_2Cl_4$ in a 10 mm tube. HDMS (hexamethyldisiloxane) was used as internal reference.

The spectra were recorded on a Bruker NMR Advance 400 spectrometer operating at 100.58 MHz (^{13}C) in the PFT mode working at 103 °C. The applied conditions were the following: 10 mm probe, 90° pulse angle; 64 K data points; acquisition time 5.56 s; relaxation delay 20 s; 3 to 4 K transient. Proton broadband decoupling was achieved with a 1D sequence using bi_waltz_16_32 power-gated decoupling.

Gradient-assisted 2D HSQC spectra were acquired with a 5 mm PFG probe operating at 103 °C.

Two dimensional NMR parameters: 90° pulse widths for ^{1}H and ^{13}C were 9.25 and 14.00 μs, respectively; relaxation delay 3.0 s.

gHSQC experiments were carried out with a delay of 1.92 ms corresponding to $^1J_{CH}$ = 130 Hz, for the creation of antiphase magnetization; 1.04 kHz as spectral width in the ^{1}H dimension and 7.04 in the ^{13}C dimension. Data were zero filled and weighted with a shifted sine bell function before Fourier transformation.

Calculation of Diad and Triad Distributions and Reactivity Ratios. The triad distributions were calculated in the reference 18, and the diad distributions were derived from triads. The analytical derivation of the reactivity ratios is described in the Supporting Information.

DSC. Measurements were performed on a Pyris 1 Perkin-Elmer instrument. The samples (∼8 mg) were heated from 50 to 250 at 20 °C/min with a nitrogen flow (30 mL/min). A first scan was realized to erase the thermal history of each polymer. T_g was then recorded during a second thermal cycle. In some cases, it was necessary to begin with the experiment at a lower temperature; then, the instrument could be cooled by means of liquid nitrogen, and the initial point was set at −40 °C.

Molar Mass Measurements. Molar masses measurements were performed on ∼12 mg of product in *o*-dichlorobenzene at 145 °C by a GPCV2000 high-temperature SEC system from Waters (Millford, MA) equipped with two online detectors: a viscometer (DV) and a differential refractometer (DRI). The column set was composed of three mixed TSK-Gel GMHXL-XT columns from Tosohaas. The universal calibration was constructed from 18 narrow MMD polystyrene standards, with the molar mass ranging from 162 to 5.48 $\times 10^6$ g mol^{-1}.

Acknowledgment. We thank Mr. G. Zannoni for his valuable cooperation in NMR analysis.

Supporting Information Available: Analytical derivation of the reactivity ratios. This material is free of charge via the Internet at http://pubs.acs.org

References and Notes

(1) (a) Kaminsky, W.; Bark, A.; Arndt, M. *Macromol. Chem. Macromol. Symp.* **1991**, *47*, 83–93. (b) Cherdron, H.; Brekner, M.-J.; Osan, F. *Angew. Makromol. Chem.* **1994**, *223*, 121–133. (c) Arndt, M.; Kaminsky, W. *Macromol. Symp.* **1995**, *97*, 225–246. (d) Kaminsky, W.; Arndt-Rosenau, M. In *Metallocene-Based Polyolefins*; Scheirs, J., Kaminsky, W., Eds; Wiley: Chichester, U.K., 2000; p 89 and references therein.

(2) (a) Ruchatz, D.; Fink, G. *Macromolecules* **1998**, *31*, 4674–4680. (b) Herfert, N.; Montag, P.; Fink, G. *Makromol. Chem.* **2001**, *94*, 3167–3182.

(3) McKnight, L. A.; Waymouth, M. R. *Macromolecules* **1999**, *32*, 2816–2825.

(4) Harrington, B. A.; Crowther, D. J. *J. Mol. Catal.* **1998**, *128*, 79–84.

(5) (a) Tritto, I.; Boggioni, L.; Sacchi, M. C.; Locatelli, P. *J. Mol. Catal. A: Chem.* **1998**, *133*, 139–150. (b) Provasoli, A.; Ferro, D. R.; Tritto, I.; Boggioni, L. *Macromolecules* **1999**, *32*, 6697–6706. (c) Tritto, I.; Marestin, C.; Boggioni, L.; Zetta, L.; Provasoli, A.; Ferro, D. R. *Macromolecules* **2000**, *33*, 8931–8944. (d) Tritto, I.; Marestin, C.; Boggioni, L.; Brintzinger, H. H.; Ferro, D. R. *Macromolecules* **2001**, *34*, 5770–5777. (e) Thorshaug, K.; Mendichi, R.; Tritto, I.; Trinkle, S.; Friedrich, C.; Mülhaupt, R. *Macromolecules* **2002**, *35*, 2903–2911. (f) Tritto, I.; Boggioni, L.; Ferro, D. R. *Macromolecules* **2004**, *37*, 9681–9693. (g) Tritto, I.; Boggioni, L.; Zampa, C.; Ferro, D. R. *Macromolecules* **2005**, *38*, 9910–9919.

(6) (a) Arndt-Rosenau, M.; Beulich, I. *Macromolecules* **1999**, *32*, 7335–7343. (b) Arndt, M.; Beulich, I. *Macromol. Chem. Phys.* **1998**, *199*, 1221–1228.

(7) Tritto, I.; Boggioni, L.; Ferro, D. R. *Coord. Chem. Rev.* **2006**, *250*, 212−241 and references therein.

(8) See http//www.topas.com and Brekner, M.-J.; Osan, F.; Rohrmann, J.; Antberg, M., Process for the Preparation of Chemically Homogeneous Cycloolefin Copolymers. U.S. Patent 5,324,801, **1994**.

(9) Recent progress: (a) Li, X.; Baldamus, J.; Hou, Z. *Angew. Chem., Int. Ed.* **2005**, *44*, 962–965. (b) Ravasio, A.; Zampa, C.; Boggioni, L.; Tritto, I.; Hitzbleck, J.; Okuda, J. *Macromolecules* **2008**, *41*, 9565–9569. (c) Marconi, R.; Ravasio, A.; Boggioni, L.; Tritto, I. *Macromol. Rapid Commun.* **2009**, *30*, 39–44. (d) Terao, H.; Iwashita, A.; Ishii, S.; Tanaka, H.; Yoshida, Y.; Mitani, M.; Fujita, T. *Macromolecules* **2009**, *42*, 4359–4361. (e) He, L. P.; Liu, J. L.; Li, Y. G.; Liu, S. R.; Li, Y. S. *Macromolecules* **2009**, *42*, 8566–8570. (f) Yang, X. H.; Wang, Z.; Sun, X. L.; Tang, Y. *Dalton Trans.* **2009**, 8945–8954. (g) Wang, B.; Tang, T.; Li, Y.; Cui, D. *Dalton Trans.* **2009**, 8963–8969. (h) Lin, Y. C.; Yu, K. H.; Huang, S. L.; Liu, Y. H.; Wang, Y.; Liu, S. T.; Chen, J. T *Dalton Trans.* **2009**, 9058–9067. (i) Ravasio, A.; Boggioni, L.; Tritto, I.; D'Arrigo, C.; Perico, A.; Hitzbleck, J.; Okuda, J. *J. Polym. Sci., Part A: Polym. Chem.* **2009**, *47*, 5709–5719.

(10) Henschke, O.; Köller, F.; Arnold, M. *Makromol. Rapid Commun.* **1997**, *18*, 617–623.

(11) (a) Boggioni, L.; Bertini, F.; Zannoni, G.; Tritto, I.; Carbone, P.; Ragazzi, M.; Ferro, D. R. *Macromolecules* **2003**, *36*, 882–890.

(b) Carbone, P.; Ragazzi, M.; Tritto, I.; Boggioni, L.; Ferro, D. R. *Macromolecules* **2003**, *36*, 891–899. (c) Boggioni, L.; Tritto, I.; Ragazzi, M.; Carbone, P.; Ferro, D. R. *Macromol. Symp.* **2004**, *218*, 39–50.
(12) Boggioni, L.; Zampa, C.; Ravasio, A.; Tritto, I.; Ferro, D. R. *Macromolecules* **2008**, *41*, 5107–5115.
(13) Hasan, T.; Ikeda, T.; Shiono, T. *Macromolecules* **2005**, *38*, 1071–1074.
(14) Kaminsky, K.; Derlin, S.; Hoff, M. *Polymer* **2007**, *48*, 7271–7278.
(15) For selectivity and reactivity in propene polymerization with metallocene catalysts, see: Resconi, L.; Cavallo, L.; Fait, A.; Piemontesi F. *Chem. Rev.* **2000**, *100*, 1253−1345 and references therein.
(16) Carvill, A.; Tritto, I.; Locatelli, P.; Sacchi, M. C. *Macromolecules* **1997**, *30*, 7056–7062.
(17) Forsyth, J.; Perena, J. M.; Benavente, R.; Perez, E.; Tritto, I.; Boggioni, L.; Brintzinger, H. H. *Macromol. Chem. Phys.* **2001**, *202*, 614–620.
(18) Boggioni, L.; Ravasio, A.; Boccia, A. C.; Tritto, I.; Ferro D. R., *Macromolecules*, **2010**, *43*, xxxx.
(19) (a) Hamm, G. E. In *Copolymerization*; Hamm, G. E., Ed.; Wiley Interscience: New York, 1964. (b) Odian, G. *Principles of Polymerization*, 3rd ed.; Wiley & Sons: New York, 1991; pp 455−458.
(20) Galimberti, M.; Piemontesi, F.; Baruzzi, G.; Mascellani, N.; Camurati, I.; Fusco, O. *Macromol. Chem. Phys.* **2001**, *202*, 2029–2037.
(21) Karssenberg, F. G.; Piel, C.; Hopf, A.; Mathot, V. B. F.; Kaminsky, W. *J. Polym. Sci., Part B: Polym. Phys.* **2005**, *44*, 747–755.
(22) Karssenberg, F. G.; Wang, B.; Friederichs, N.; Mathot, V. B. F. *Macromol. Chem. Phys.* **2005**, *206*, 1675–1683.
(23) Herfert, N.; Montag, P.; Fink, G. *Makromol. Chem.* **1993**, *194*, 3167–3182.
(24) Tritto, I.; Boggioni, L.; Jansen, J. C.; Thorshaug, K.; Sacchi, M. C.; Ferro, D. R. *Macromolecules* **2002**, *35*, 616–623.
(25) (a) Heatley, F.; Salovey, R.; Bovey, F. A. *Macromolecules* **1969**, *2*, 619–623. (b) De Marco, A.; Sozzani, P.; Di Silvestro, G.; Farina, M. *Macromolecules* **1989**, *22*, 2154–2156.
(26) Busico, V.; Cipullo, V. *J. Am. Chem. Soc.* **1994**, *116*, 9329–9330.
(27) Yoder, J. C.; Bercaw, J. E. *J. Am. Chem. Soc.* **2002**, *124*, 2548–2555.